JETIR.ORG ISSN: 2349-5162 | ESTD Year : 2014 | Monthly Issue
JOURNAL OF EMERGING TECHNOLOGIES AND INNOVATIVE RESEARCH (JETIR)
An International Scholarly Open Access, Peer-reviewed, Refereed Journal

CONTROLLING OF SOLAR BASED ELECTRIC VEHICLE CHARGING STATION THROUGH INTELLIGENT CONTROLLER FOR G2V AND V2G MODES

[1]K.VINOD KUMAR, [2]DR.M.BALASUBBA REDDY,

[1]PG Scholar, Department of EEE, Chaitanya Bharathi Institute of Technology Gandipet, Hyderabad
[2]Professor, Department of EEE, Chaitanya Bharathi Institute of Technology Gandipet, Hyderabad

Abstract : Electric cars are often charged with power that is mostly generated from fossil fuels, which is often cited as an argument against transport electrification being considered clean. Solar-powered EV charging stations are expanding and promising to provide true green mobility, despite research showing that transportation electrification, regardless of power source, lowers carbon emissions and air pollution. These EV charging stations are eco-friendly since they use solar panels to produce power. The maximum power of a PV module varies with temperature, solar radiation, and load, making it one of the most challenging concerns. In order to determine the MPPT, this research builds a PV array, DC-DC converter, and fuzzy logic controller into a Simulink model and runs simulations. The state-of-charge (SOC) of electric vehicles is found to be high after just a brief period of charging. In this article, the EV's DC connection is tied into the single-phase grid and the PV system is equipped with a Fuzzy controller and maximum power point tracking. When a PV array is not available, electric vehicle is charged from the power grid. A 660V boost converter is used to charge a 100AH battery from the PV array panel. The voltage is then regulated to accommodate a buck circuit that requires a 220 V battery. DC-DC boost converter and bidirectional converter are linked to the electric vehicle for charging and discharging, and a bidirectional AC-DC rectifier is connected to power grid. During the charging and discharging processes, the EV battery's voltage and current are shown. Voltage and current from the grid are perfectly in sync during charging. Discharging is said to throw them out of phase, indicating the direction of power is backward.

IndexTerms **- Solar-power, PV array, DC-DC converter, state-of-charge (SOC), AC-DC rectifier, Fuzzy controller, maximum power point tracking, EV battery.**

I. INTRODUCTION

Rising fuel prices and pollution limitations call for novel technological solutions in daily life. The automobile industry has a perpetual obligation to its patrons to provide top-notch service. Engineers are looking at ways to make this happen in the hopes that electric vehicles will become the dominant mode of transportation in the future. Electric vehicle (EV) batteries may be charged using solar energy. Therefore, the strain and complexity of the system are reduced when EVs are incorporated into solar EV charging stations referred from[1]. Consequently, a solar-powered EV charging system is presented in this study. In Figure 1, an EV is seen charging from both the grid and solar panels. The electric vehicle (EV) is charged by solar photovoltaic (PV) panels when the sun is out, and by the utility grid when the sun isn't out. To get the most out of the solar panels even when they are partially shaded, MPPT techniques are used to adjust the duty ratios of the Boost converter connected to the PV array. The quantity of energy produced by PV array is dependent on volume of sunlight available and the ambient temperature [1]. An MPPT method was developed in this study by following the MPPT of a PV system with a fuzzy logic controller [3]. The 660V output voltage is generated by the Fuzzy controller and used to charge the 100AH system batteries from the PV array panel. To accommodate the 220 V battery requirement, the voltage is stepped down for buck operation. Under a wide range of conditions, Matlab/Simulink shows that the SOC represents fully charged in a relatively short length of time. Solar photovoltaic panels and a DC-DC boost converter make up first stage of this plant model's EV charging infrastructure, while an AC-DC converter linked to grid and EV's DC-DC bidirectional converter make up the second.

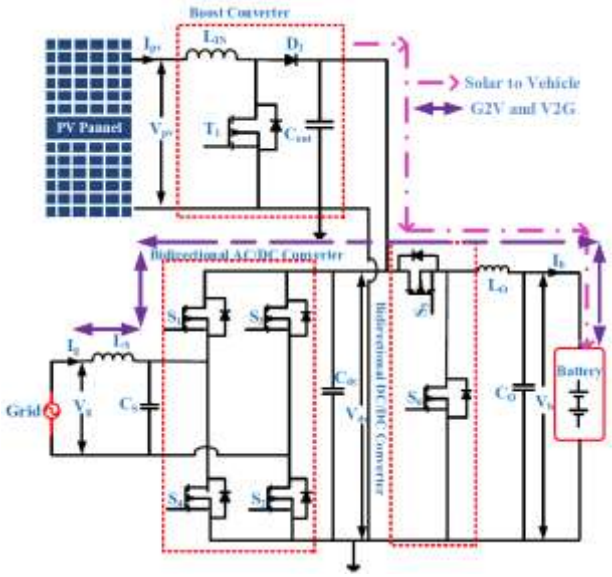

Figure 1. Solar-powered electric vehicle charging setup

II. PV Array Mathematical Modeling Analysis

A. VOLTAGE OF THE OPEN-CIRCUIT

The greatest voltage drawn from a PV array with zero current is known as the VOC or open-circuit voltage. Light-generated current is biassed towards the PV cell junction, which in turn increases the open-circuit voltage.

$$V = \frac{NKT}{Q} in \frac{I_L - I_o}{I_o} + 1Volt$$

whereas open-circuit voltageV, diode ideality constant N, Boltzmann constant was denoted (1.381*10^-23 J/K) was denoted as K, the temperature in Kelvin was denoted as T, electron charge (1.602*10^-19 c) was denoted as Q, the solar-generated current was denoted as Iph(A), and the saturation diode current was denoted as Io(A).

B. RADIATION LIGHT-GENERATED CURRENT

$$I_L = \frac{G}{G_{ref}} * \left(I_{Lref} + \propto I_{sc}\left(T_c - T_{cref}\right)\right)$$

The temp coefficient of a short-circuit current (A/K) = 0.0065/K ISC, and current produced by light (radiation) (IL), whereas radiation (W/m2) G, radiation 1000 W/m2Gref, photoelectric current 0.15 An ILref, module temperature 298 KTCref, and the temperature of the light source (G).

C. REVERSE SATURATION CURRENT

$$I_o = I_{or} * (\frac{T}{T_{ref}})^3 e^{\left(\left(\frac{QE_g}{KN}\right)*\left(\frac{1}{Tr} - \frac{1}{T}\right)\right)}$$

$$I_{or} = \frac{I_{sc}}{e^{\left(V_{ocn}/NV_{tn}\right)}}$$

Whereas reverse saturated current Io, saturation currentI_{or}, ideality-factor 1.5 N, and band gap for silicon 1.10 eVE_g.

D. CURRENT OF THE SHORT-CIRCUIT

When the I_{sh} = IL. Then from it maximum current is produced by the PV cell. Due to short circuit operation: V = 0.

$$I_{sh} = I_L - I_o\left(\left(e^{\left(Q\frac{V - IR_S}{NKT}\right)} - 1\right)\right)$$

III. MPPT Controller Using Fuzzy

DC/DC converters employ MPPT extraction devices to adjust output voltage of the PV array to maintain an optimum power output. The MPPT is determined by the fuzzy MPPT controller once PV array's output voltage and current have been measured. Fuzzy controller output alters DC/DC converter's trigger PWM duty cycle waveform.

$$E(k) = \frac{P(k) - P(k-1)}{V(k) - V(k-1)}$$

$$\Delta E(k) = E(k) - E(k-1)$$

where *P*(*k*) and *V*(*k*) are instant power and the voltage respectively of PV array generator.

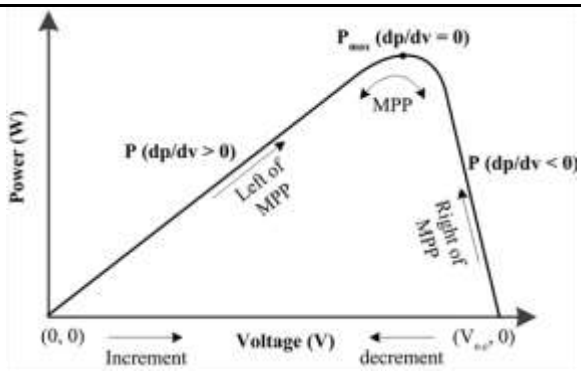

Figure 2. Fuzzy logic controller theory for maximum power point tracking.

The MPPT makes use of the FLC Mamdani method. The FLC uses Fuzzification, an Inference Engine, and Defuzzification to achieve its goals.

IV. DESIGN AND CONFIGURATION OF THE EV CIRCUIT

A. Boost Converter

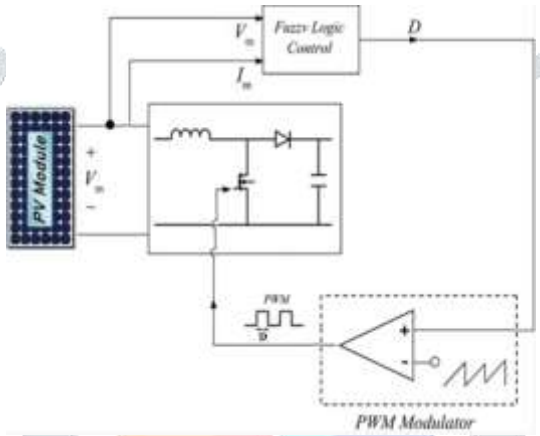

Figure 3. A DC-DC converter with a fuzzy controller is linked to the PV array.

To increase and control the PV array's output voltage, the system incorporates PV panels wired to a boost converter. To get the most out of your PV system, use an MPPT FLC controller. Figure 1 provides a block schematic of the proposed system. DC-DC boost converters include a high frequency switch (MOSFET), an inductor, and a diode for freewheeling, and its primary function is to increase the input voltage to the desired output voltage. Magnitude of the voltage on the output side is larger than the voltage applied. The output voltage is controlled by the control strategies employed to run the duty cycle of the MOSFET. When the MOSFET is closed, the PV array is used to charge the inductor. The freewheeling diode limits the current flow to the DC link capacitor from the source. The diode is forward biased when the MOSFET is turned on. The capacitor is charged by the PV array and an inductor connected to the discharges.

B. Bi-Directional Controller Concept

To reduce complexity and ensure system stability during the mode shift of the Bidirectional converter, a unified controller is suggested. Using a buck and boost controller, as shown in Figure 3 (a), is a common example of a current mode controller in action. The transition between the two states is managed by an energy-savings command. The indicator of the mode being used is the direction of the current flow, with positive for the charging current in buck mode and negative for the discharging current in boost mode. Here the sole way to control charging and discharging is by setting iL0*, the reference current, to a positive or negative value.

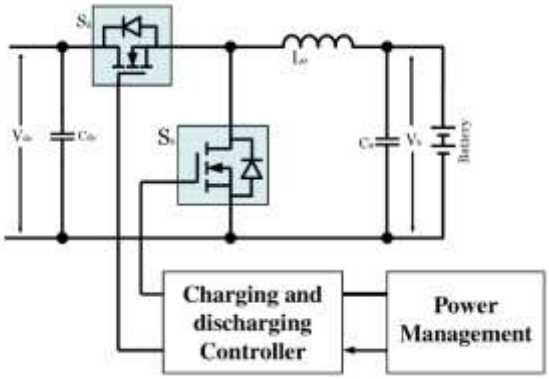

Figure4. The Bidirectional converter's power stage was managed by the PWM controller.

For complicated, non-linear systems subject to load disturbance and uncertainty, Fuzzy logic controllers may give a robust response. These controllers use a flexible if-then structure. These controllers are gaining popularity for controlling bidirectional DC-DC converters because of their flexibility. The key benefit of this approach is that it requires fewer measurements to build the controller than the sliding control approach does, and it does not need any previous knowledge of the system's characteristics. Both voltage control mode controller models and the system's steady-state and transient response are analysed in MATLAB Simulink. Based on

simulation results, the FLC system outperformed the PI and PR controllers in terms of response stability, dynamic range, and time to stabilise. The EV battery voltageV_b, inductor-currentI_{L0}, and duty cycle d are all calculated using this DC model. Since the power plant transfer function is the same for the both buck charging and the boost discharging, the single controller can govern both. The direction of flow of the average current through the designated inductor, iL0, is the same as that of power used to charge the EV battery. The action between duty cycle D (control) and zero current duty cycles S5 and S6 has (zero current) determined the direction of current flow in I_{L0}. In order to charge the EV battery, the average current through inductor, shown by the symbol I_{L0}, must be larger than zero. The same holds true for duty cycle D, which should be raised to greater than D_0.

V. RESULTS AND DISCUSSION

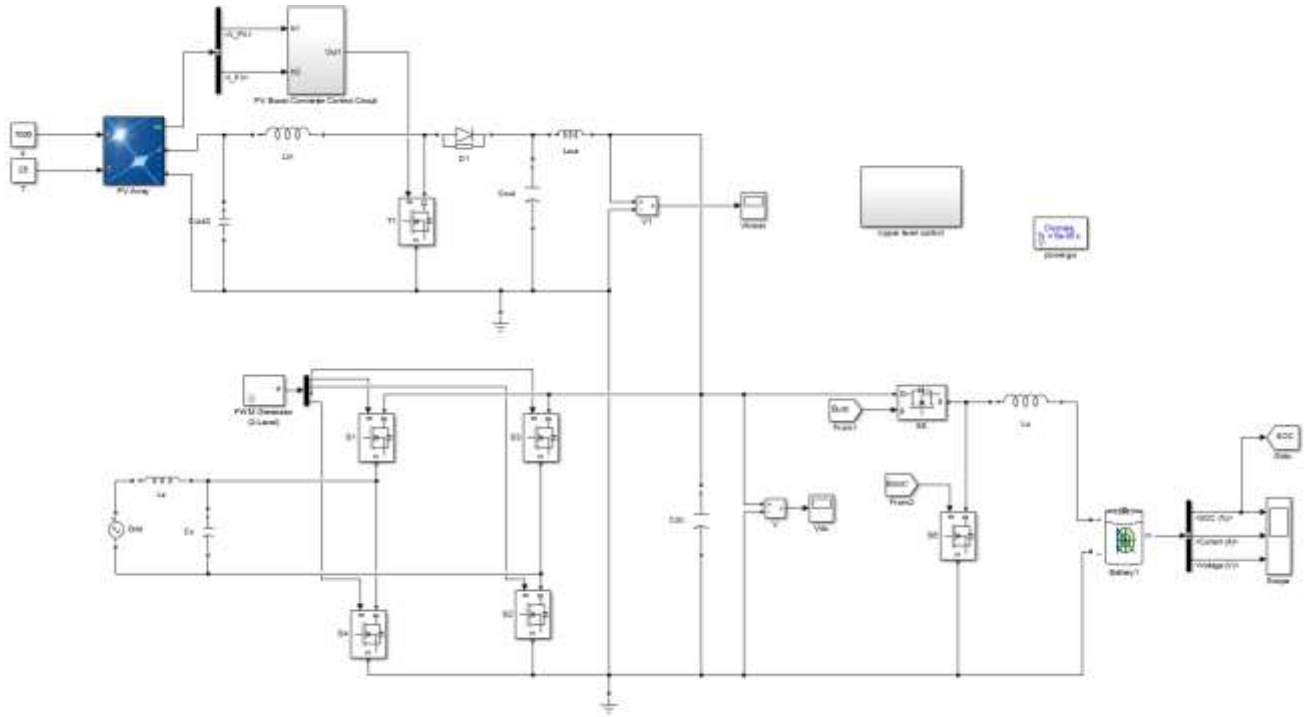

Figure5. Simulation Diagram of the EV with Solar Charging System.

The EV battery is charged by the PV array electricity throughout the daytime. The voltage of a PV panel may be increased by a boost converter to between 200 and 660 volts. A 230V, 100AH, (20 kWH) battery is used herein. The in-vehicle charging system may be installed in garages and parking garages.

Case 1: Grid to Vehicle.

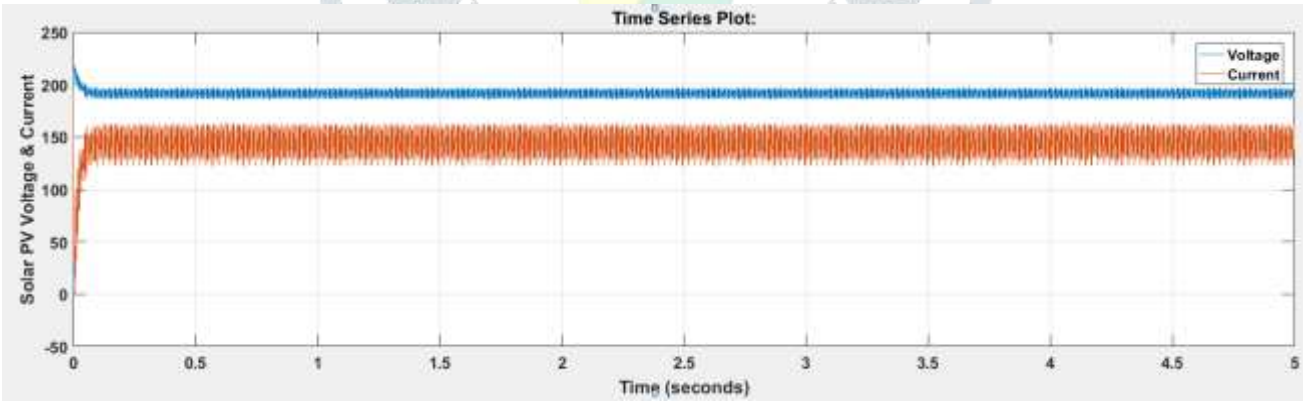

Figure6. Multiple-Phase-Power-Tracking-Regulator (MPPT) for Solar-Powered Arrays.

Approximately 200V is generated by a PV array array. There is a 0.9% steady state error0.2% and it takes the PV array 0.122s to follow the MPPT reference voltage (Vmppt). The boost converter in Figure 6 produces 660V at its output. Battery in Fig. 7 we see the battery current and voltage. FIGURE 8: The charge level of the EV battery while it is being charged.

Solar PV MPPT voltage tracking time for the PV array is 0.022 seconds. Figure 7 shows the 660V output of the boost converter. Battery voltage and current are shown in Figure 9. The charging process for an electric vehicle is shown in Figure 8.

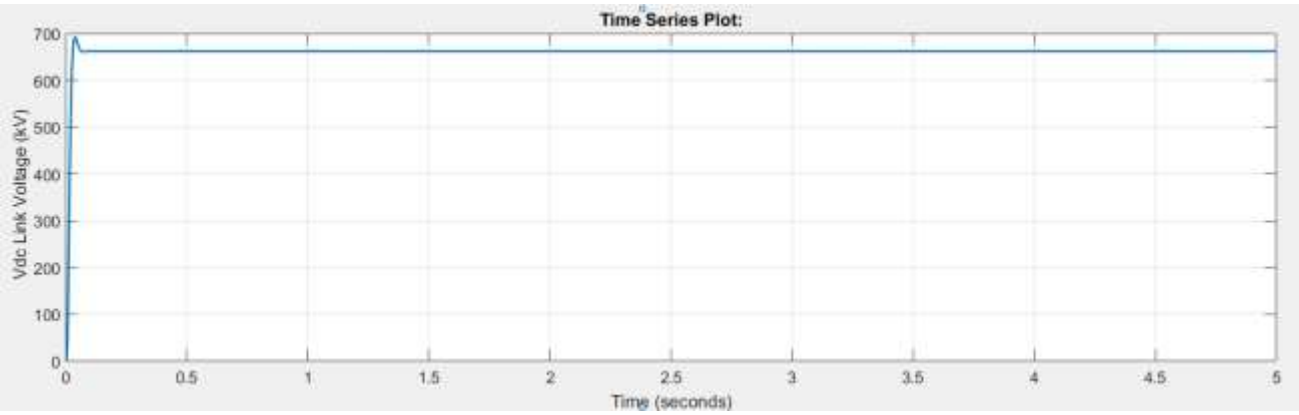

Figure7. Boost Converter Output DC Voltage

DC link Voltage of the boost converter is 660V.

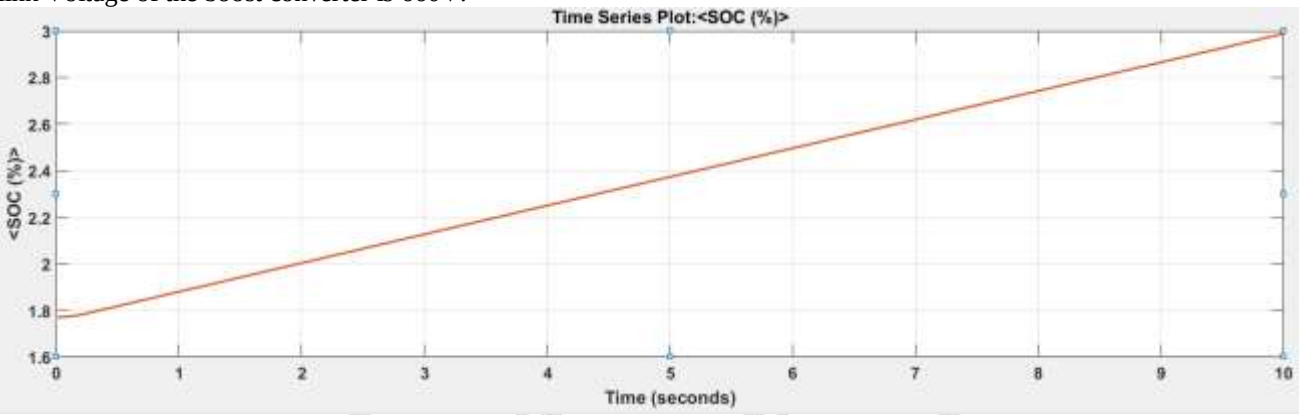

Figure8. State of Charge of the EV Battery during charging

State of Charge during the charging of the EV from the minimum value.

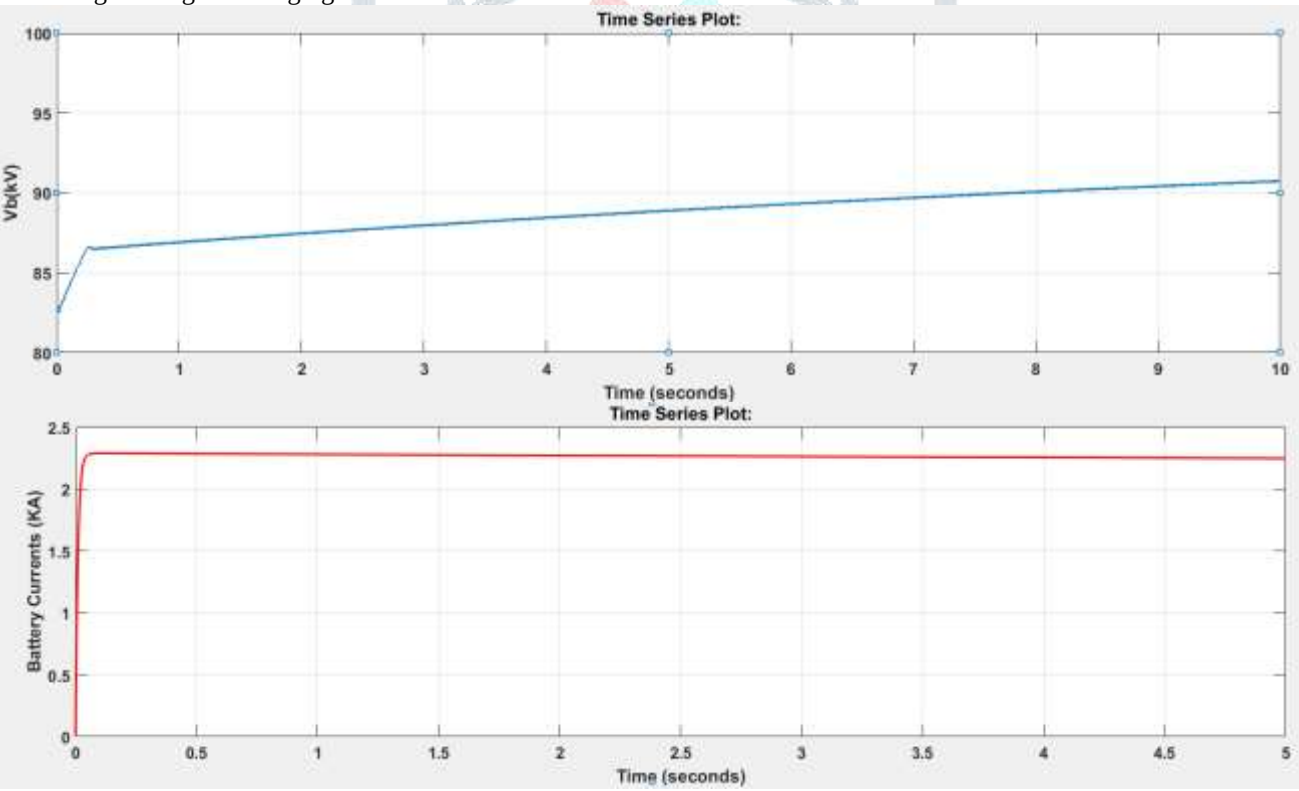

Figure9.Battery charging Voltage and Current

Case 2: Vehicle to grid

The inverter, which is an AC-DC bidirectional converter, modulating grid current at its output. In response to grid demands and at the discretion of the EV owner, the battery supplies electricity to the grid. In order to charge an electric vehicle, a bidirectional AC-DC converter is subjected to switching pulses. Here, input current and voltage are in phase with one another. The voltage waveform of a charging battery is seen above, while the current waveform stays constant. The state-of-charge waveform is shown when the battery is being charged. Odd order harmonics are present in grid voltage and current during charging.

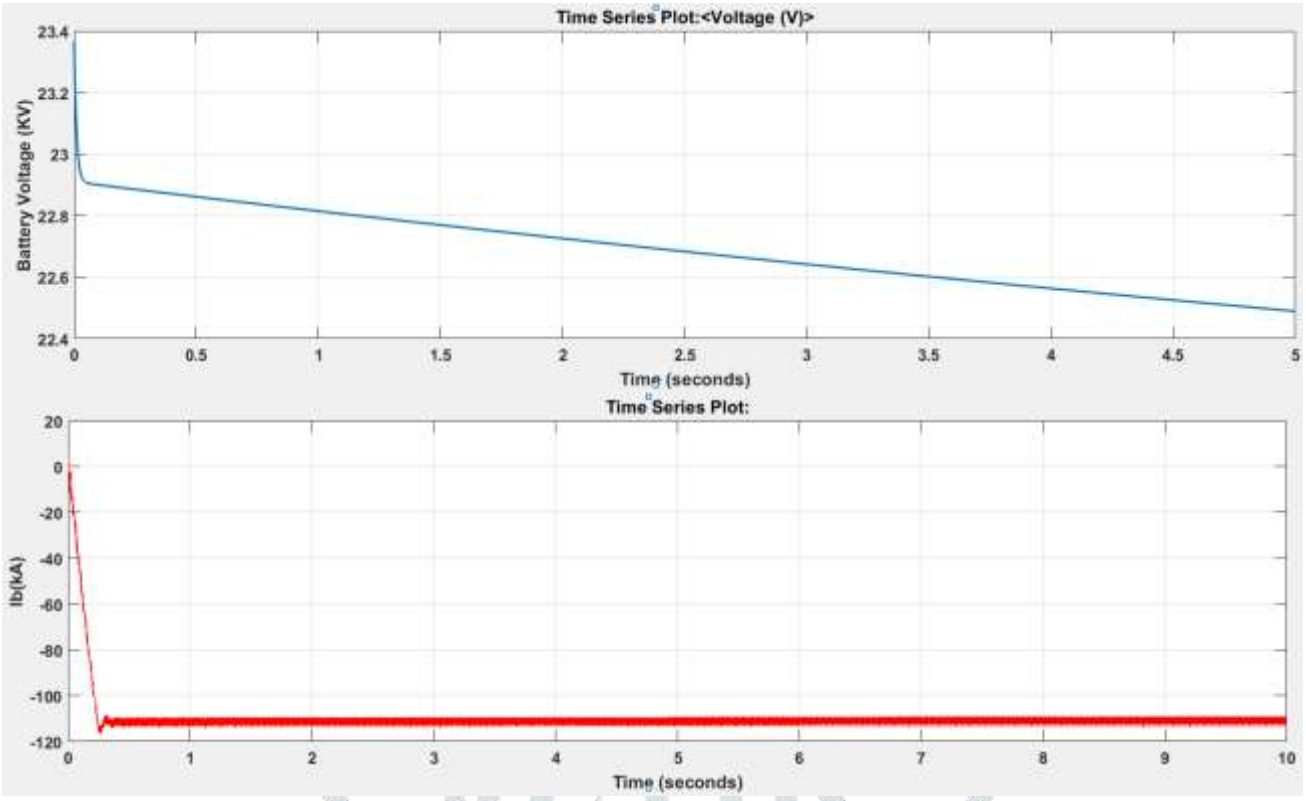

Figure10. Battery discharging Voltage and Current

Discharging causes the grid voltage and current waveforms to be antiphase (fig.12). It's a visual representation of the power flow from an EV battery to the grid. While the current waveform stays constant during battery discharge, both the voltage and current waves diminish. Discharging battery state of charge (SOC) is seen in fig11.

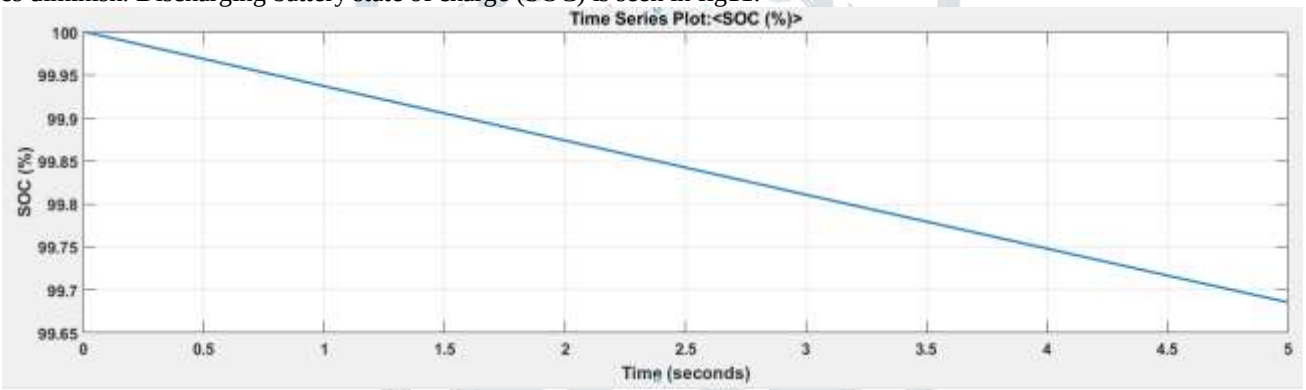

Figure11. Discharging SOC of the EV

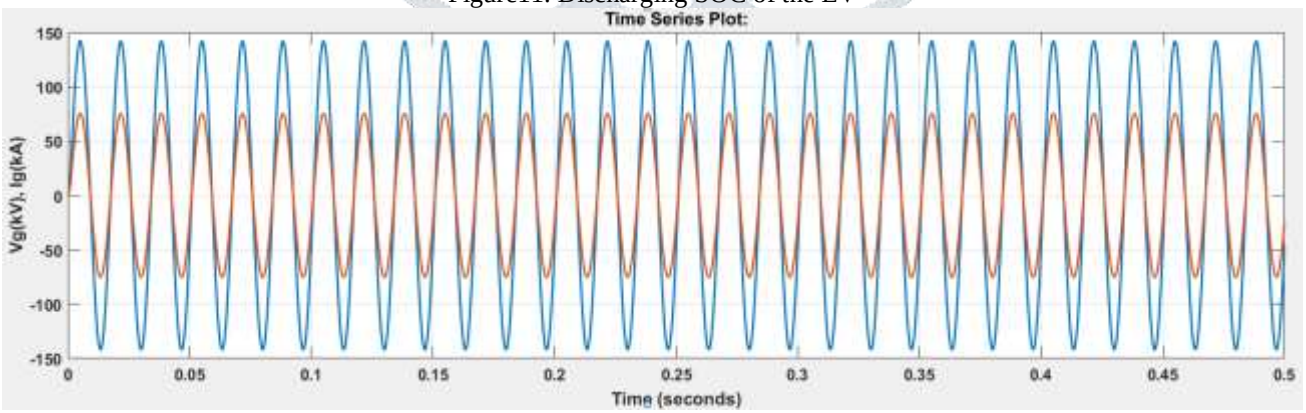

Figure12. Grid Voltage and Current waveforms.

CONCLUSION

The 200-volt output voltage of the PV system is boosted to 400-volts through a boost converter. To adapt to the dynamic needs of an electric vehicle's battery, a buck converter filters the output voltage and steps it down. To achieve the aforementioned objectives, a fuzzy-based MPPT system is used to represent mathematical architecture of PV array system and to simulate the PV system in different climatic scenarios. The battery charging and discharging processes, as well as the performance of the fuzzy-based MPPT system, are analysed. Both charging and discharging modes have been proven to effectively improve the EV battery SOC performance. The frequency response characteristic was used to determine that a corner frequency of 10 rad/s was optimal. To illustrate how electric vehicles (EVs) connect to and disconnect from the grid, we may look at the voltage and current are out of phase which has a unity power factor. The suggested unified controller works well in the high-power DC-DC bidirectional converter. The steady functioning has been verified by load stepping experiments in both buck charging and boost draining modes. The findings validate proposed model and validate its potential use in the design of a unified controller to maintain a

consistent charging and discharging current. Charging PV arrays mitigates voltage difficulties in the distribution network brought on by more generators and higher electricity demand from recharging electric vehicles.

APPENDIX

Table 1 PARAMETERSOF THE CIRCUIT CONFIGURATION

Circuit Variables	Ratings
Frequency	F=60 Hz
Grid voltage	Vg=120 V rms
AC capacitor Filter	Cs=20 µF
AC inductor Filter	Ls=0.75 mH
Inductor	Lo=41µH
DC Capacitor Cdc	2 mF
Battery capacity	Ib=100AH
Capacitor Co	600 µF
PR Controller parameters Kp, Γi	100, 0.1ms
Hysteresis bandwidth h	±0.5 V

Table 2. PV BOOST CONVERTERPARAMETERS

Parameters	Value
Boost converter input Voltage	Vin=200 V
Input inductor	Lin=1.3 mH
Output Voltage	Vo=400 V
Output capacitor	Cout=2500 µF
Switching frequency	10kHz
Duty ratio	0.5

Table3. PARAMETERS OF PV ARRAY

PV Array	Value
Parallel strings	50
Series connected modules per string	6
Cells per module	60
Short circuit current ISC (A)	7.84
Open circuit voltage (V)	36.3
Current at maximum power point Imp(A)	7.35
Voltage at maximum power Vmp (V)	29

REFERENCES

[1] Nian Liu, Oifang Chen, Xinvi Lu, Jie Liu and Jianhua Zhang, “A Charging Strategy for PV-Based Battery Switch Station Considering Service Availability and Self-Consumption of PV Energy,” IEEE Trans. Ind Electronics., vol.62, no.8, pp. 4878-4889, Feb 2015.

[2] K. Chaudhari, A. Ukil, K. N. Kumar, U. Manandhar and S. K. Kollimalla, “Hybrid Optimization for Economic Deployment of ESS in PV-Integrated EV Charging Stations,” IEEE Trans. Ind. Informatics, vol. 14, no. 1, pp. 106-116, Jan 2018.

[3] Bhim Singh, Anjeet Verma, A. Chandra and Kamal Al-Haddad, “Implementation of Solar PV-Battery and Diesel Generator Based Electric Vehicle Charging Station,” in IEEE International Conference on Power Electronics, Drives and Energy Systems (PEDES), 2018.

[4] Hoang N. T. Nguyen, Cishen Zhang, and Jingxin Zhang, “Dynamic Demand Control of Electric Vehicles to Support Power Grid With High Penetration Level of Renewable Energy,” IEEE Trans. Transportation Electrification, vol. 2, no. 1, pp. 66-75, Mar 2016.

[5] Xie W, Hui J. MPPT for PV system based on a novel fuzzy control strategy. In: 2010 International Conference on Digital Manufacturing & Automation; ChangSha; 2010. pp. 960-963

[6] Anandhakumar G, Venkateshkumar M, Shankar P. Intelligent controller based MPPT method for the photovoltaic power system. In: 2013 International Conference on Human Computer Interactions (ICHCI); Chennai; 2013. pp. 1-6

[7] Indumathi R, Venkateshkumar M, Raghavan R. Integration of D-Statcom based photovoltaic cell power in low voltage power distribution grid. In: IEEE-International Conference on Advances in Engineering, Science and Management (ICAESM-2012); Nagapattinam, Tamil Nadu; 2012. pp. 460-465

[8] M. C. Kisacikoglu, B. Ozpineci, and L. M. Tolbert, “EV/PHEV bidirectional charger assessment for V2G reactive power operation,” IEEE Trans. Power Electron., vol. 28, no. 12, pp. 5717–5727, Dec. 2013.

[9] By Xiaosong Hu, Chagfu Zou, Caiping Zhang, And Yang Li, “Technological Developments in Batteries” IEEE power& energy magazine, pp. 20- 31, Sep/Oct 2017.

[10] X. Zhou, S. Lukic, S. Bhattacharya, and A. Huang, “Design and control of grid-connected converter in Bi-directional battery charger for plugin hybrid electric vehicle application,” in Proc. IEEE Veh. Power and Propulsion Conf., pp. 1716–1721, Sep 2009.

[11] D.N. Zmood, D.G. Holmes, “Stationary frame current regulation of PWM inverters with zero steady-state error,” IEEE Trans. Power Electron, vol. 18, no.3, pp. 814-822, May 2003.

[12] A.V.J.S.Praneeth, Najath A Azeez, Lalit Patnaik, Sheldon S Williamson, ‘‘Proportional Resonant Controllers in On-board Battery Chargers for Electric Transportation,’’ IEEE International Conference on Industrial Electronics for Sustainable Energy Systems (IESES). pp. 237-242, 2018.

[13] De Brito, M.A.G., Junior, L.G., Sampaio, L.P., Melo, G.A.E. and Canesin, C.A. (2011) Main Maximum Power Point Tracking Strategies Intended for Photovoltaics. XI Brazilian Power Electronics Conference, Natal, 11-15 September, 524-530.

[14] Sahu, P., Sharma, A. and Dey, R. (2020) Ripple Correlation Control Maximum Power Point Tracking for Battery Operated PV Systems: A Comparative Analysis. 2020 IEEE International IOT, Electronics and Mechatronics Conference, Vancouver, 9-12 September 2020, 1-6.

[15] Trivedi, A., Gupta, A., Pachauri, R.K. and Chauhan, Y.K. (2017) Comparison of Perturb & Observe and Ripple Correlation Control MPPT Algorithms for PV Array. 2016 IEEE 1st International Conference on Power Electronics, Intelligent Control and Energy Systems, Delhi, 4-6 July 2016, 1-5.

[16] Belkaid, A., Colak, U. and Kayisli, K. (2017) A Comprehensive Study of Different Photovoltaic Peak Power Tracking Methods. 2017 IEEE 6th International Conference on Renewable Energy Research and Applications, San Diego, 5-8 November 2017, 1073-1079.

[17] Ibnelouad, A., El Kari, A., Ayad, H. and Mjahed, M. (2017) A Comprehensive Comparison of the Classic and Intelligent Behavior MPPT Techniques for PV Systems. 2017 14th International Multi-Conference on Systems, Signals & Devices, Marrakech, 28-31 March 2017, 526-531.

[18] Hamed, B.M and El-Moghany, M.S. (2012) Fuzzy Controller Design Using FPGA for Photovoltaic Maximum Power Point Tracking. International Journal of Advanced Research in Artificial Intelligence, 1, 14-21.

[19] Ali, A.I.M., Mohamed, E.E.M. and Youssef, A.R. (2018) MPPT Algorithm for Grid-Connected Photovoltaic Generation Systems via Model Predictive Controller. 2017 Nineteenth International Middle East Power Systems Conference, Cairo, 19-21 December 2017, 895-900.

[20] Samosir, A.S., Gusmedi, H., Purwiyanti, S. and Komalasari, E. (2018) Modeling and Simulation of Fuzzy Logic Based Maximum Power Point Tracking (MPPT) for PV Application. International Journal of Electrical and Computer Engineering, 8, 1315-1323.